MEASUREMENTS OF CHANGES OF PHOTOELECTRIC PROBABILITY FACTOR DUE TO SURFACE CONTAMINATION OF ALUMINUM

by

RICHARD LEE PERRY

A THESIS

submitted to

OREGON STATE COLLEGE

in partial fulfillment of
the requirements for the
degree of

MASTER OF SCIENCE

June 1955

APPROVED:

Redacted for Privacy

Professor of Physics

In Charge of Major

Redacted for Privacy

Chairman of Department of Physics

Redacted for Privacy

Chairman of School Graduate Committee

Redacted for Privacy

Dean of Graduate School

Date thesis is presented 6/10/54

Typed by Ruth Perry

ACKNOWLEDGEMENT

The author takes this opportunity to express his appreciation to Dr. J. J. Brady for suggesting this problem, and for his help and constructive criticism during the project. He also thanks Frank Collins, the glassblower of the Linfield College Physics Department, for an excellent job of constructing the experimental tube. The assistance given by the author's wife, Ruth, in correcting grammar and typing the thesis is greatly appreciated.

TABLE OF CONTENTS

TABLE OF FIGURES

MEASUREMENTS OF CHANGES OF PHOTOELECTRIC PROBABILITY FACTOR DUE TO SURFACE CONTAMINATION OF ALUMINUM

INTRODUCTION

The photoelectric effect was the subject of much investigation from about 1930 to about 1940. Previous to 1930, the theories used to describe and predict what actually takes place were very inadequate.

In 1931, R. H. Fowler (5, pp. 45-56) developed his theory of spectral distribution, which predicts quite accurately the form of the spectral distribution of the photoelectrons in the vicinity of ν_o, the threshold frequency. Fowler built his theory around the fact that in experimental work on ordinary metals, the highest frequency in the ultraviolet that is usually available to the experimentalist does not exceed the threshold frequency by more than 50 percent. Therefore the experimentalist is primarily interested in a theory that is reasonably accurate in the vicinity of the threshold frequency.

If the theory is to be confined to the vicinity of the threshold, there are a number of considerations that become evident. The first of these is that the electrons which can be ejected from the metal are only those whose initial energies lie within a few percent of the maximum energy allowed by the Fermi-Dirac statistics. Since these are just the electrons that are most strongly affected by temperature changes, temperature effects are important, and it is not permissible to carry out the calculations as though the surface were at 0°K.

Since the initial velocities of the electrons that are ejected lie in a relatively small range, any probability factors which depend on a small power of the initial velocity may be considered as essentially constant. Therefore the probability function may be considered as a constant.

Since the frequency range to be considered is also small, factors depending on a small power of the frequency ν will be relatively unimportant compared to factors involving $(\nu-\nu_o)$, where ν_o is the threshold frequency.

Another basic idea used by Fowler is that the photoelectric effect is essentially a surface phenomenon. Using this idea, it is unnecessary to try to determine, as was attempted previously, how much energy an electron loses between the time it absorbs a photon and the time it reaches the surface of the metal. The assumption is made that only those electrons will be emitted whose energy, which is their initial energy plus $h\nu$, is greater than the surface potential step.

If N_b is the number of electrons per second coming up to unit area of surface with the initial energy sufficient to make them available for ejection, then the photoelectric current I is

$$I = \alpha e N_b$$

where e is the electronic charge, and α is a proportionality factor, which is assumed constant over the frequency range, involving the

probability of an electron absorbing a quantum when unit intensity of radiation falls on the surface.

This may be rewritten into the form

$$I = \alpha A T^2 \phi(x)$$

where T is the absolute temperature, A is the universal constant $\frac{4\pi mek^2}{h^3}$, h is Planck's constant, k is the Boltzmann constant, m and e are the mass and charge of the electron, and $\phi(x)$ is a universal function of $x = \frac{h(\nu-\nu_o)}{kT}$.

This theory is very useful in the analysis of experimental data by graphical means if it is rewritten into the form

$$\log_{10} \frac{I}{T^2} = B + \Phi(x)$$

where $B = \log_{10} \alpha A$ = constant, and $\Phi(x) = \log_{10} \phi(x)$. Experimental values of $\log_{10} \frac{I}{T^2}$ are plotted against x, giving a set of curves. These curves should be the same for all metals and all temperatures except for an additive constant, and they should be superposable on the theoretical curve obtained by plotting $\Phi(x)$ against x.

L. A. DuBridge (4, pp. 727-741) used the methods of Fowler's theory to investigate the problem of the energy distribution of photoelectrons when the frequency of the incident light is held

constant. The most general case is the problem of the distribution of the total energies of the emitted photoelectrons. This includes velocity components parallel to the emitting surface as well as the components normal to the emitting surface.

The equation developed for the photoelectric current for the case involving the distribution of total energies is

$$I = \alpha A T^2 \Psi(x, x_o)$$

where $\Psi(x, x_o)$ is a universal function of x and x_o. If V is the applied retarding potential, $x = \frac{Ve}{kT}$ and $x_o = \frac{V_m e}{kT} = \frac{h(\nu-\nu_o)}{kT}$ where $V_m = \frac{h(\nu-\nu_o)}{e}$ is the retarding potential required to stop the most energetic of the emitted photoelectrons.

If $(x-x_o) > 1$ and $x_o > 10$, this equation may be rewritten in the form

$$\log_{10} \frac{I}{xT^2} = B + \chi(x-x_o)$$

where $B = \log_{10} \alpha A$ and $\chi(x-x_o) = \log_{10} \left[e^{-(x-x_o)} - \frac{1}{4} e^{-2(x-x_o)} + \cdots \right]$

A theoretical curve is obtained when $\chi(x-x_o)$ is plotted against (x_o-x). The experimental curves, which should be superposable on the theoretical curve, are obtained by plotting $\log_{10} \frac{I}{xT^2}$ against -x.

The horizontal shift required to superpose the experimental curves on the theoretical curve should equal x_o, and therefore V_m may be determined. The vertical shift necessary should be equal to B, and α can be determined from this shift.

There has been very little investigation of α up to the present time and therefore very little is known about it. The object of this experiment was to determine whether α changes when the emitting surface is changed. In this case an aluminum emitter was studied with varying degrees of oxygen contamination. Since it is easier to vary the retarding potential than to vary the frequency of incident radiation, the theory of the distribution of total energies was used in this experiment.

Aluminum was chosen because Thein (9, pp. 287-292) found large changes in the work function as aluminum became contaminated.

Mann and DuBridge (6, pp. 120-124) made an attempt to detect any change in α for contamination of beryllium, but they reported that no conclusions could be drawn from their data.

APPARATUS

In order to measure the total energy of the emitted electrons, it is necessary that they travel along the electric field lines of the retarding potential. Since the electrons may be emitted in any direction, it is then necessary to have the retarding field radial from the point of emission. This is approximated experimentally by using concentric spherical electrodes with the emitting sphere very small in comparison to the collecting sphere. Since it is necessary that the experiment be performed at a pressure of about 10^{-6} millimeters of mercury or less, it is necessary to enclose these electrodes in an evacuated tube.

The experimental tube was made from a Pyrex two liter spherical flask. The collecting electrode was made by evaporating aluminum onto the inside surface of the glass sphere. There were three aluminum evaporators arranged symmetrically around the axis of the sphere and at an angle of about 45° with the axis of the sphere.

Each evaporator (Figure 1) was made of a piece of aluminum inside of a coil of 15 mil tungsten wire. The coil was spotwelded to a two wire press seal. The two leads were 50 mil Koolite tungsten leads. Uranium glass was used between the Koolite leads and the Pyrex. Two small pieces of glass tube were loosely placed on the leads so that the evaporated aluminum would not cause an electrical short between the leads. Three evaporators were made into the tube although one would have been sufficient. This provided insurance in

case any were burned out as well as allowing the repetition of the experiment if necessary.

Electrical contact was made to the collecting electrode with three button seals arranged symmetrically about the axis of the tube between the evaporators. Three button seals were used to insure good contact with the evaporated aluminum. The button seal consisted of a Koolite lead sealed to uranium glass and the uranium glass sealed to Pyrex. A conducting silver paint was applied to the lead and the area around it. This provided a good electrical contact when the aluminum was evaporated onto it. The electrical resistance between any two of the button seals was seven ohms or less after the aluminum was evaporated.

A hollow aluminum hemispherical electrode (Figure 2) with a diameter of about two centimeters was placed in the center of the tube to serve as the emitter. A small coil of 10 mil tungsten wire was placed inside of the hemisphere to supply heat for outgassing or decontaminating the hemisphere if it became necessary to do so. The coil and the hemisphere were spotwelded to long 40 mil tungsten leads and these were spotwelded to 50 mil Koolite leads in a four wire press seal. Two small pieces of glass tubing were placed on the two central leads so that the heating coil would not be shorted out by the evaporated aluminum.

A polished quartz disk was mounted on a Pyrex to Vycor graded seal. This was placed opposite the hemispherical emitter along the axis of the tube. The quartz disk was necessary to provide a window for the ultraviolet to enter the tube. It had to be mounted

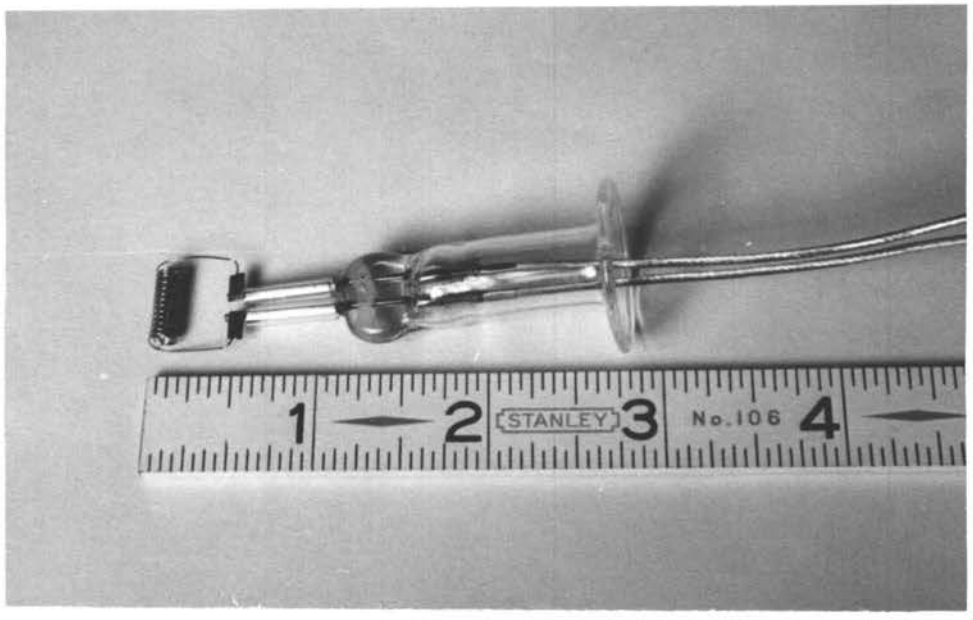

Figure 1. Aluminum Evaporator

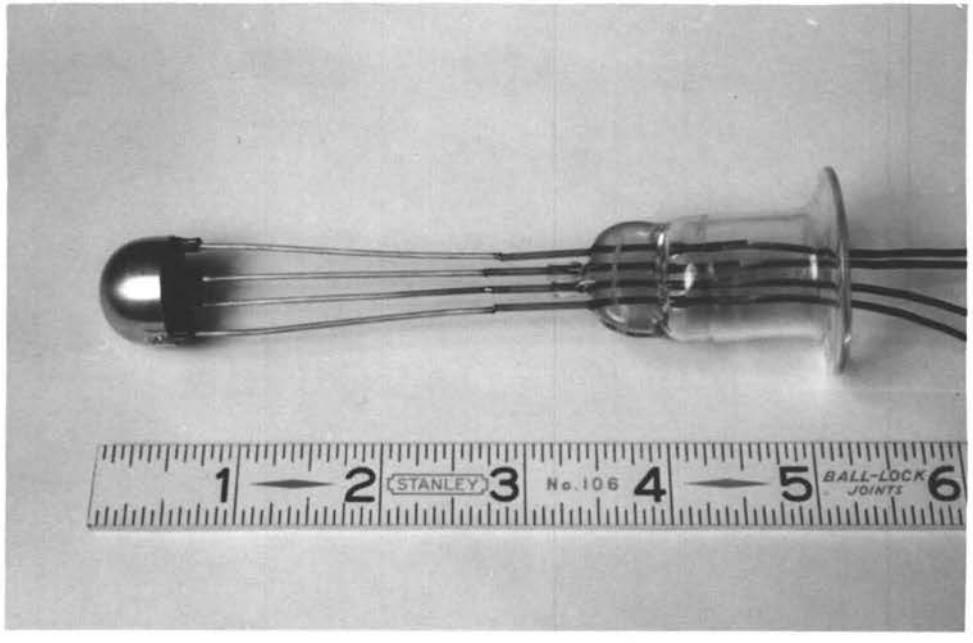

Figure 2. Hemispherical Electrode

on the graded seal so that the difference of thermal coefficient of expansion between quartz and Pyrex would not break the tube during the bakeout process.

The only quartz that was available was a larger rough sawcut disk and a smaller polished disk had to be made from it. First a smaller disk was cut from the large disk and then several pieces were cut from the remainder. The cutting tool (Figure 3) was made of a piece of copper tubing mounted on a solid shaft. The large quartz disk was mounted on a piece of wood with soft wax and a dam of Johns-Manville Duxseal was built up around it. This was filled with a light oil (water is as good) and a coarse carborundum grit. The cutting operation (Figure 4) was done in a drill press with only very slight pressure applied for short periods of time. Care was taken to keep the carborundum out of all of the machinery.

The disk was mounted with wax in the center of a flat brass plate (Figure 5) with the other pieces of quartz arranged symmetrically around it. Then a strip of masking tape was wrapped around the disk to form a container around the pieces of quartz (Figure 6). This was filled with plaster of paris and the excess was scraped off. This made a solid holder for the quartz (Figure 7). The extra pieces of quartz helped to keep the disk flat during the polishing. Wood could not be used in place of the brass disk because it changes the relative positions of pieces of quartz when it absorbs moisture and expands. Pitch also is not good for pieces this small because it flows too easily.

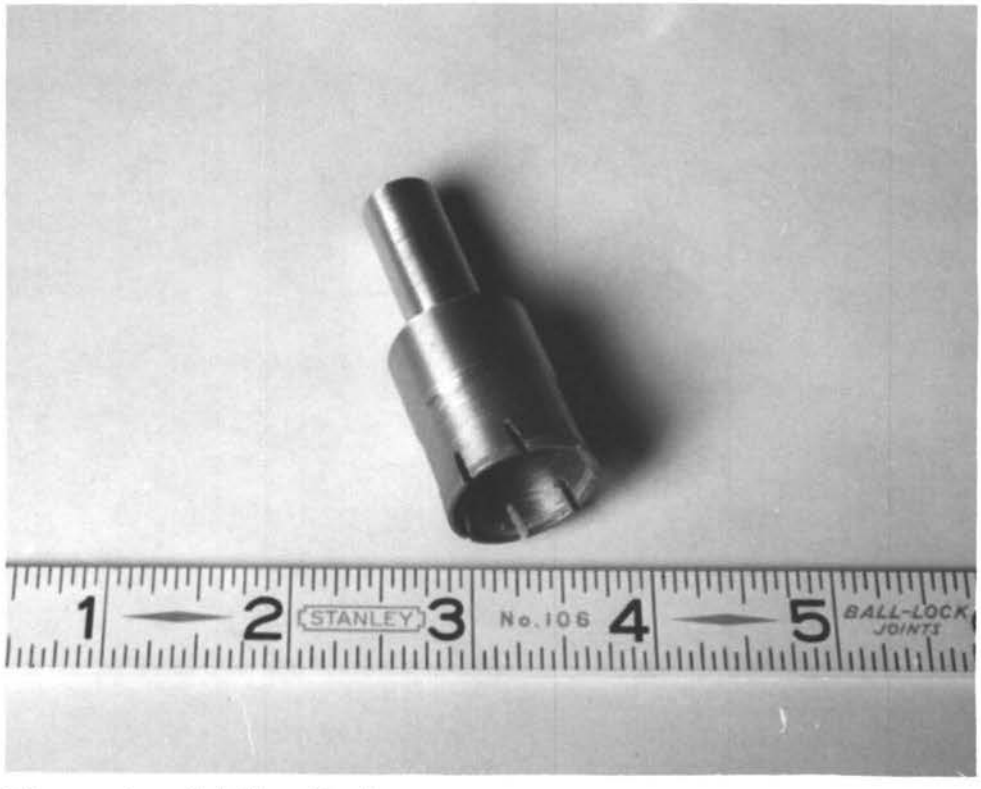

Figure 3. Cutting Tool

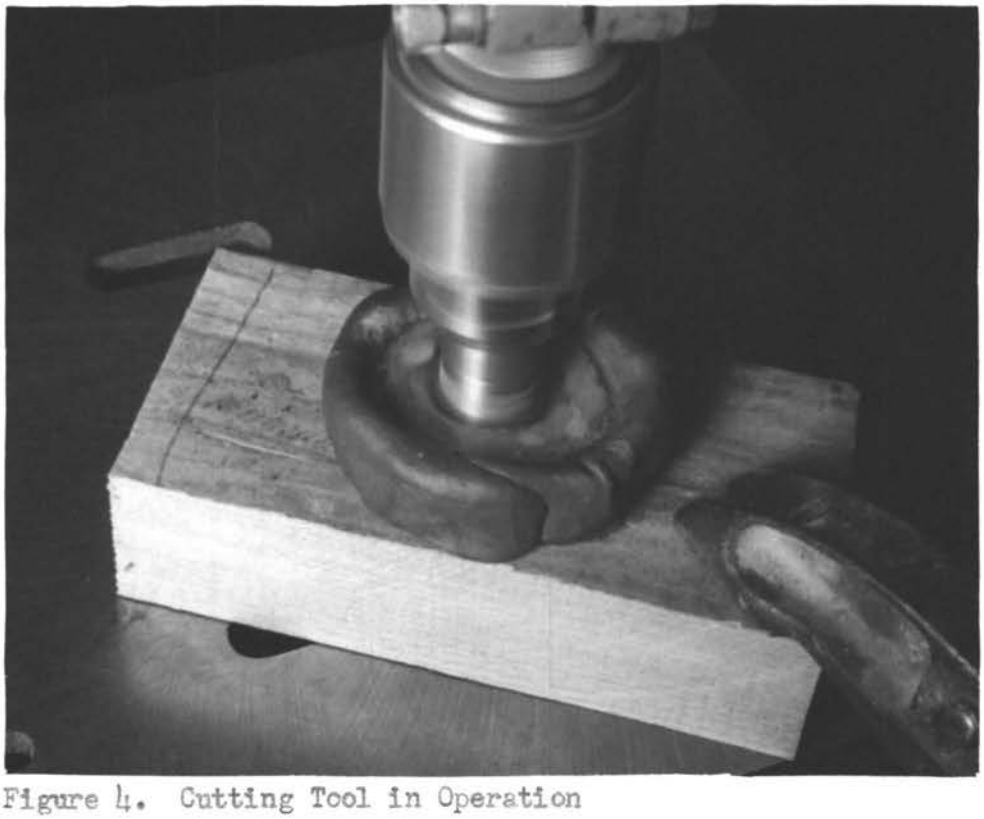

Figure 4. Cutting Tool in Operation

Figure 5. Brass Plate

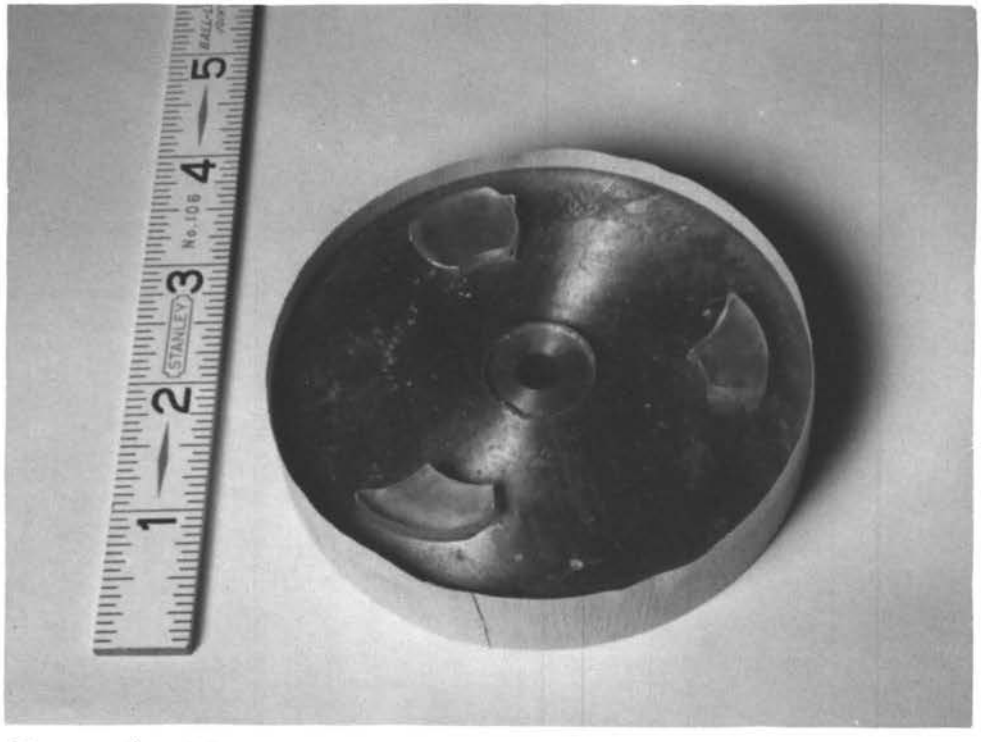

Figure 6. Pieces of Quartz Mounted on Brass Plate

The fast grinding was done on a machine driven iron lap (Figure 8) with coarse carborundum mixed with a little water. Finer and finer grits were used in quick succession since the grinding went so fast at this point. Care was taken to keep the grits from getting mixed, in order to prevent scratches.

The next step was to use a piece of quarter inch plate glass as the lap. Care was taken to place it on a flat surface so that it would stay flat, and also to keep it clean of grit. A thin paste of water and a fine abrasive powder was put on it. The quartz was rubbed over this paste covered glass surface with a completely random motion (Figure 9). As this smoothing process continued, it became possible to see a slight reflection at a grazing angle of incidence. Then all surfaces were thoroughly washed and a finer powder was used for the paste. It was necessary to be very careful to keep grits and small chips of quartz from scratching the surfaces.

Before starting to polish this side of the quartz, the brass plate was heated until the wax melted and then the pieces of quartz and plaster of paris were turned over as a unit so that the two sides of the disk would be more nearly parallel. When the wax had hardened, the grinding and smoothing processes were repeated for the second side.

When the smoothing process was completed, the disk was removed from the plaster of paris and thoroughly cleaned. It was polished on a piece of felt placed on a flat surface with a paste of water and cerium oxide on the felt. The disk was held as shown in Figure 10

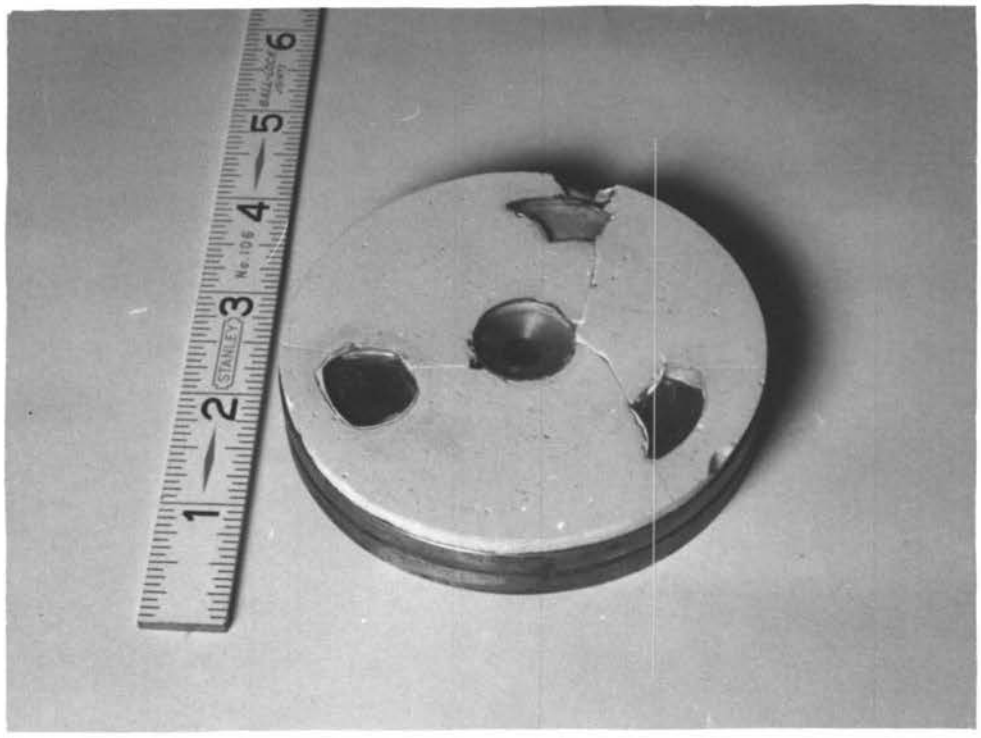

Figure 7. Quartz Holder with Plaster of Paris Added

Figure 8. Grinding Process with Machine Driven Iron Lap

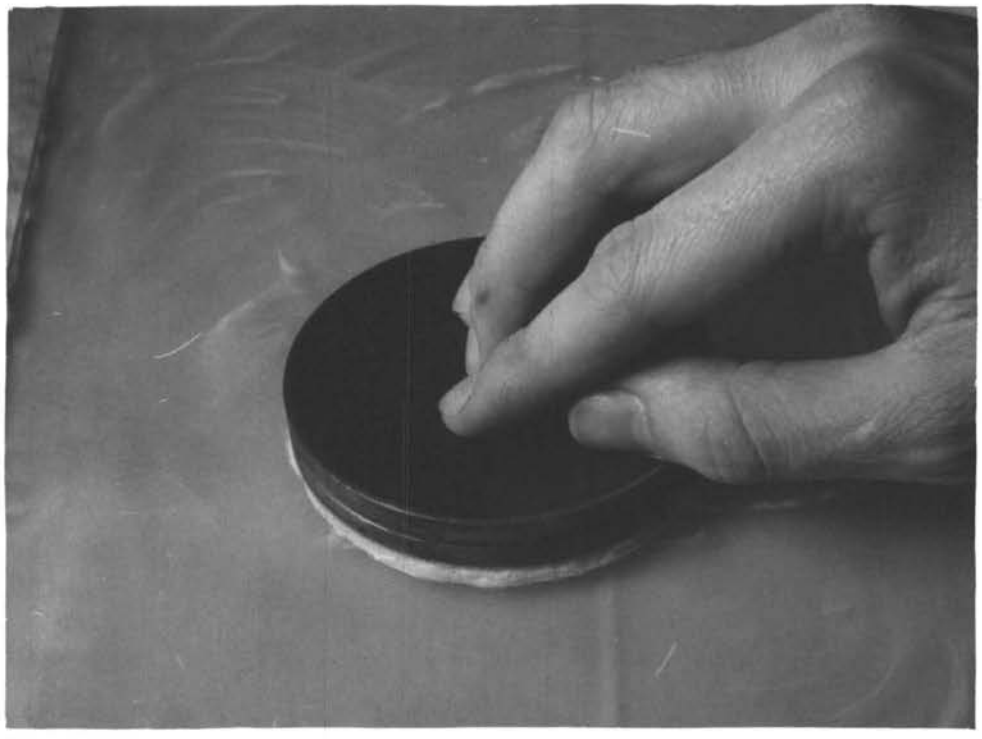

Figure 9. Smoothing Process on a Glass Plate

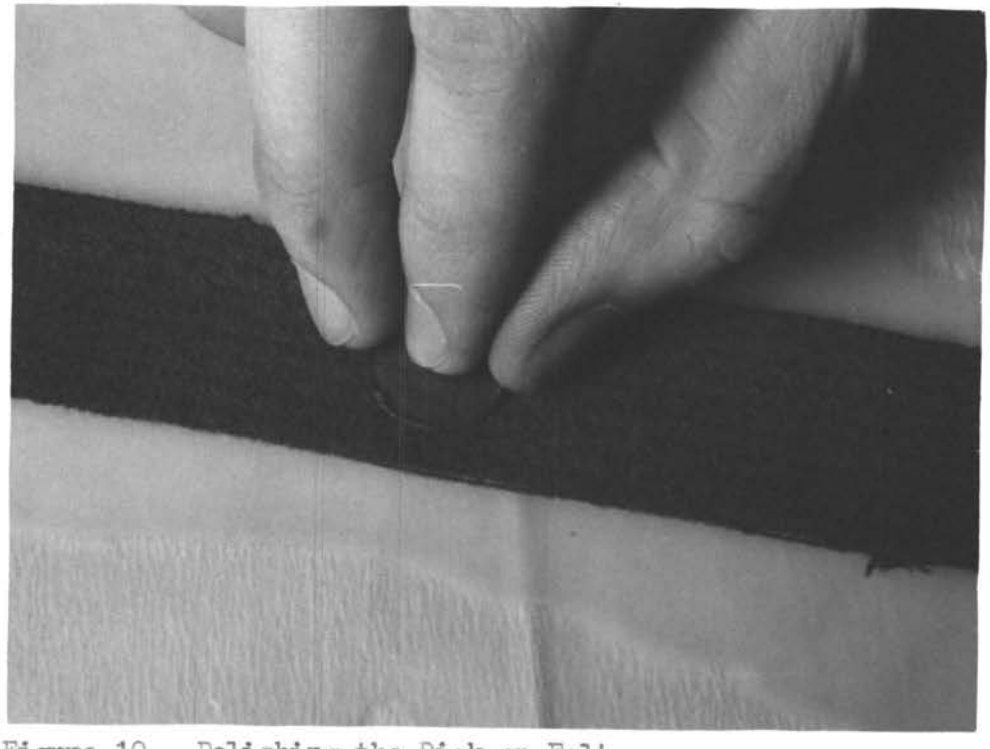

Figure 10. Polishing the Disk on Felt

instead of being mounted on some type of holder because the holder tends to increase the probability of deviation from a flat surface. Care was taken to keep the fingers from rubbing on the felt after it started to rub the skin off. The completed disk was clear and sufficiently flat. The surfaces were slightly rough, somewhat like the surface of a lemon. This may have been caused by the felt.

The window was sealed to the Vycor side of the graded seal with a small and very hot flame.

Two views of the completed tube are shown in Figures 11 and 12. Figure 11 is a side view of the tube taken at an angle of about 90° with the axis of the tube. Figure 12 was taken at an angle of about 30° with the axis of the tube, which passes through the center of the tube and through the center of the quartz window, which is in the upper lefthand corner of each figure. The open tube at the lower righthand corner of each figure was the connection between the tube and the vacuum system.

The tube was sealed onto the portable vacuum system, which was built on a four wheel cart. The mechanical fore pump was a Cenco Megavac. An Eimac three stage oil diffusion pump was connected in series with the fore pump.

A cold trap was mounted between the experimental tube and the oil diffusion pump. A suggestion by Alpert (1, pp. 1004-1005) was tried out, involving the placing of a roll of corrugated copper foil inside of the cold trap to increase the surface area and reduce the mean free path of the air molecules in the trap. Since there were

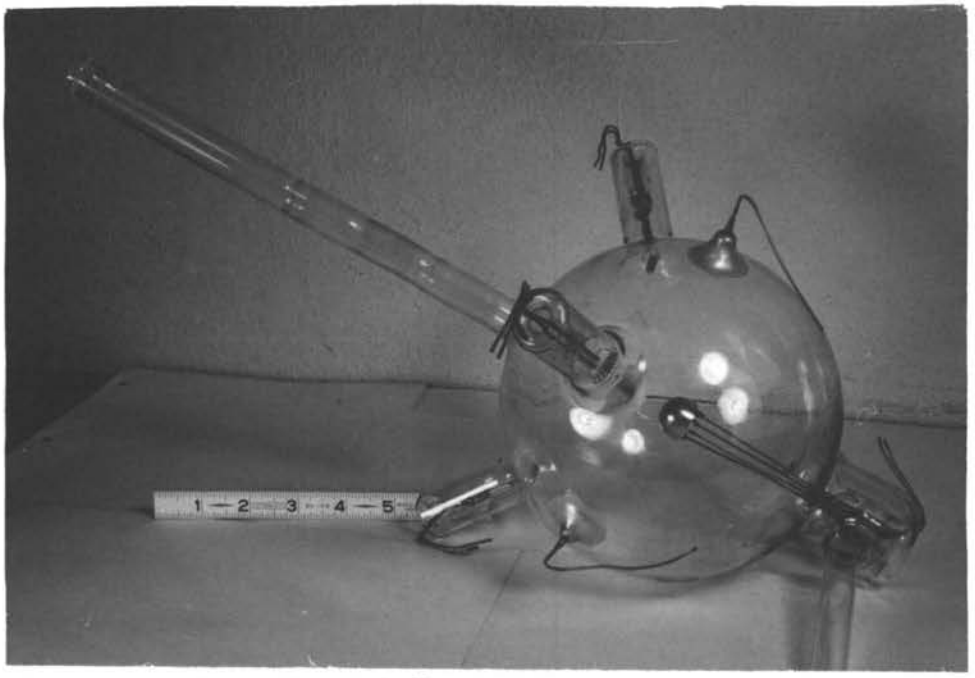

Figure 11. Experimental Tube

Figure 12. Experimental Tube

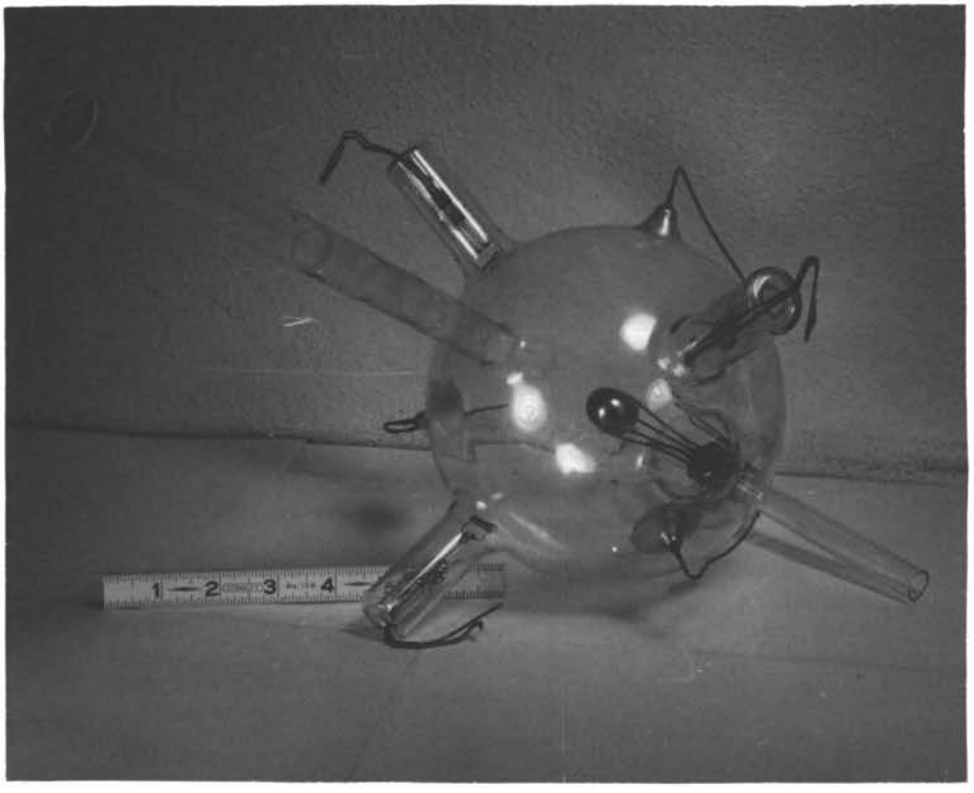

no rollers available to corrugate the copper, plaster of paris was poured onto a piece of corrugated cardboard. When it had set, the cardboard was removed and the copper foil was pressed into the corrugated plaster of paris. Then the corrugated copper foil was rolled up together with a piece of smooth copper foil, thus forming a large number of small even sized passageways.

Three vacuum gauges were used with the system. A National Research Corporation type 501 thermocouple gauge was mounted between the fore pump and the oil diffusion pump. There were two Distillation Products, Inc. ionization gauges mounted on the high vacuum side of the diffusion pump. A type VG-2 ionization gauge was mounted between the diffusion pump and the cold trap. Its rating, as given by the manufacturer, was 32 microamperes per micron of pressure. A type VG-1A ionization gauge was mounted between the cold trap and the experimental tube. Its rating was 100 microamperes per micron. The electrical circuits for operating these gauges were already constructed, but an RCA type WV-84A direct current micro-ammeter was placed in the plate circuit to get accurate measurements of the plate current.

Two ovens were built to bake out the tube and the cold trap during the evacuation process. The oven for the cold trap was made from a piece of stainless steel tubing 2-1/4 inches in diameter and 13 inches long. Glass tape was wrapped around the tube to provide electrical insulation. Then a 110 volt, 1000 watt replaceable heating element was wound around this and fastened to terminals

mounted on pieces of Transite at each end of the tube. Several coats of Sauereisen liquid porcelain were then applied to cover up the heating element. Asbestos paper was shredded up, soaked in water with sodium silicate added, packed around the tube and coils, and baked on. Several layers of asbestos paper were wrapped around this and fastened on with a steel strap. A piece of asbestos paper was rolled up and inserted into the tube to keep the hot metal from coming into direct contact with the glass walls of the cold trap. A thermocouple was placed inside to indicate the temperature. This oven was mounted in a vertical position on a piece of Transite covered with a layer of asbestos. It was a simple operation to raise it up and around the trap. This oven brought the temperature of the trap from room temperature up to 400°C in about an hour with 60 volts applied to the heating element.

The oven for the tube was built up like a box around the tube. The bottom of the oven was a piece of 1/2 inch Transite 21 inches long and 14-1/2 inches wide. The sides and top were pieces of 1/4 inch Transite 14-1/2 inches wide and 19-1/2 inches long. The two ends were pieces of 1/4 inch Transite 15 inches long and 14 inches wide. Three 110 volt, 1000 watt heating elements were used, one on each of the sides and the top. They were fastened to the Transite with two turns of Nichrome wire at about every three inches. Small pieces of Transite were inserted between the element and the large piece of Transite to keep the large piece from cracking because of high temperature changes. The bottom piece was raised about 1/2 inch

to provide an air space between it and the top of the cart. Four holes were drilled in it and four 1/2 inch steel rods 16-1/2 inches long with threads on each end were inserted and bolted down. These were posts to which the sides, ends, and top were fastened. An asbestos blanket was draped over the oven to help keep the heat in. A 400°C thermometer was inserted near the top of the oven. With 110 volts applied to each of the three heating elements, it took about 1-1/4 hours to raise the temperature inside the oven from room temperature to 400°C.

The light source was a Sun-Kraft model A-1 cold quartz ultraviolet ray therapy lamp. It was not possible to limit the light source to one wavelength, but an approximation was made. The photoelectric threshold frequency of aluminum is about 2840 Angstrom units, so any light of wavelength greater than this has no effect. The transmission qualities of the quartz used for the window and also a quartz lens used for focusing the light on the emitter are such that frequencies below 1800 or 1900 Angstrom units will not be transmitted. Also, the manufacturer's specifications on the ultraviolet lamp state that 86 percent of the intensity is in the 2537 Angstrom lines. The manufacturer did not mention any lines of shorter wavelength but his spectrum diagram does indicate lines at 2654 Angstroms and at 2800 Angstroms that may have some effect. Therefore, it was assumed that in the vicinity of the maximum retarding potential, the 2537 Angstrom line would be the only one of importance.

The intensity of the ultraviolet light source was monitored with a PJ23 gas filled photocell in series with a 90 volt battery and a direct current microammeter.

The retarding potential was applied by a Leeds and Northrup student potentiometer using two dry cells in series as a power source and a Weston standard cell with a known electromotive force for calibration. It was permissible to use the potentiometer because the currents drawn from it were so slight. The positive terminal was grounded and the negative potential was then applied to the collecting electrode.

Since the photoelectric current was so small, it had to be amplified and then passed through a very sensitive galvanometer. The current was amplified with an FP-54 Pliotron current amplifier tube. The leads from the emitting hemisphere were connected to the control grid of the amplifier tube. Since the grid needed a potential applied to it instead of a current, the current was shunted to ground through a resistance of 1.025×10^{11} ohms, thus applying the potential drop across the resistance to the control grid of the tube. The electrical circuit for the amplifier was a balanced circuit designed by DuBridge and Brown (2, pp. 532-536) to eliminate fluctuations in the output current when the 12 volt battery supplying the filament current and plate potential fluctuated. The amplifier tube, electrical circuit, and the leads between the tube and circuit were all shielded with copper. The input lead from the

experimental tube to the control grid of the amplifier tube was also shielded with copper foil.

The output of the amplifier was connected through an Ayrton shunt, to a Leeds and Northrup galvanometer with a sensitivity of about 10^{-9} amperes per millimeter deflection with a distance of one meter between the galvanometer and the ground glass scale. In this experiment, the ground glass scale was mounted at a distance of 223 centimeters from the galvanometer.

Figure 13 shows the tube after the aluminum was evaporated, mounted on the vacuum system. The VG-1A ionization gauge is just to the left and above the tube. The cold trap is in the lower left part of the picture. It hangs through a hole in the corner of the top of the cart. The vacuum pumps are underneath the top of the cart. The FP-54 Pliotron current amplifier tube is located behind the cold trap and is shielded with copper foil and a brass tube. One of the sides of the oven is in place behind the experimental tube. The way in which the heating element is fastened onto the Transite can be seen. The quartz lens is held in a clamp just to the right of the quartz window. To the right of this is located the PJ23 photocell and on the extreme right edge of the picture is one corner of the metal box housing the ultraviolet lamp.

Figure 14 shows the general experimental setup. The potentiometer circuit is located on the left side of the table in the left foreground. To the right of this is the Ayrton shunt and a resistance box for use with the shunt. The DuBridge and Brown

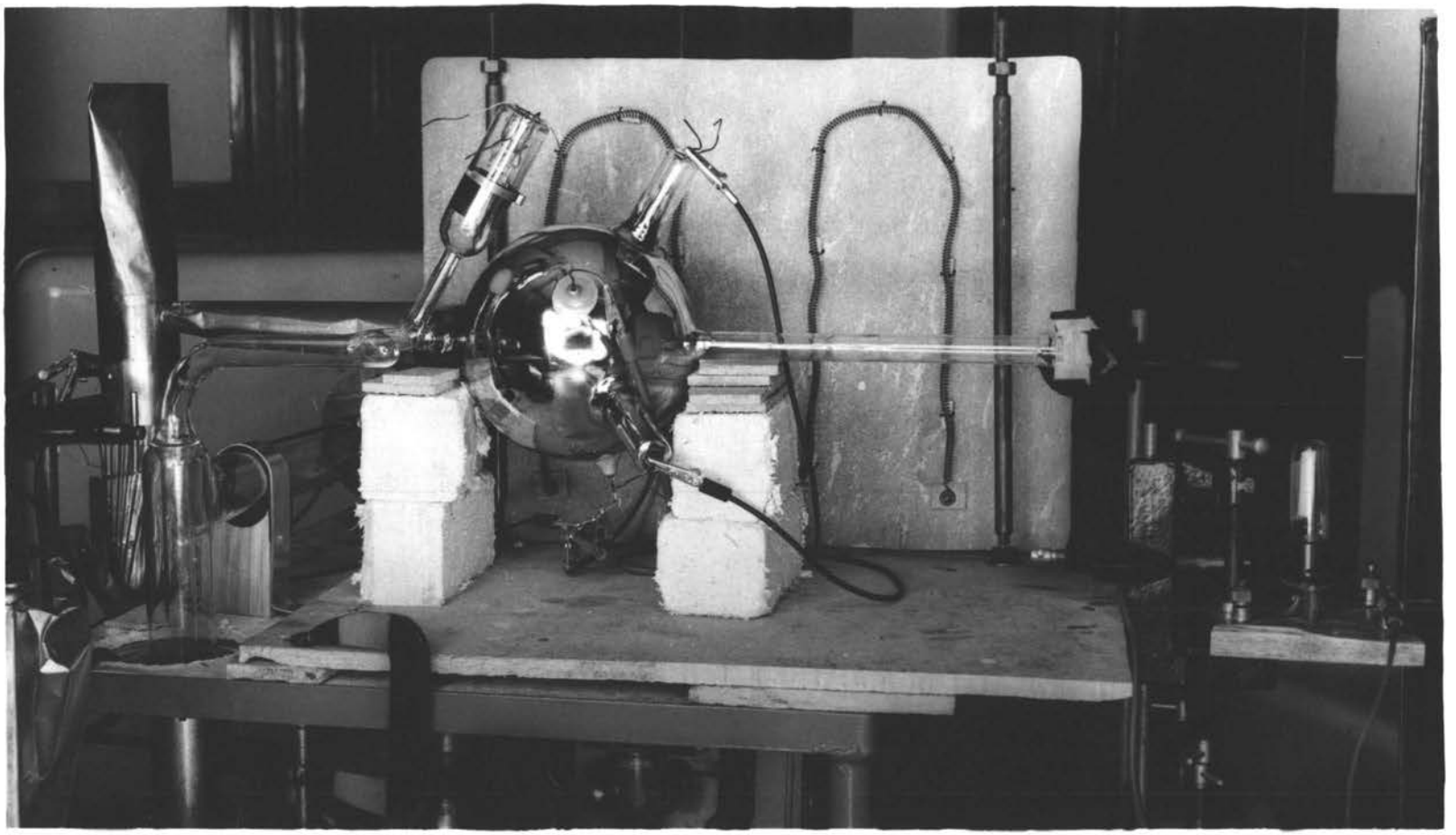

Figure 13. Experimental Tube Mounted on the Vacuum System

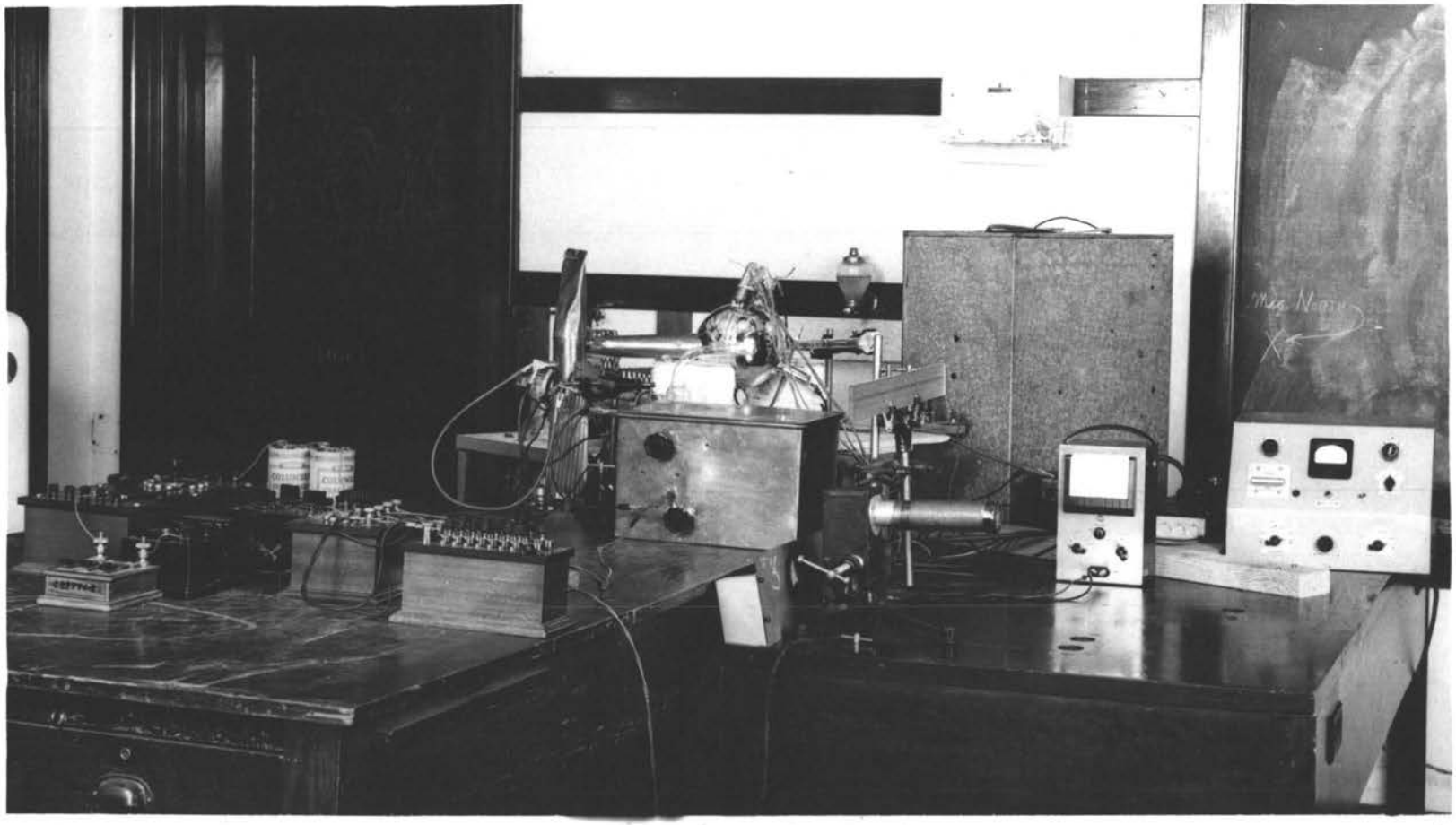

Figure 14. The Experimental Setup

balanced circuit for the FP-54 current amplifier tube is in the copper box on the right rear corner of the left table. Behind the copper box is the cart with the tube and vacuum system.

The circuit for the VG-1A ionization gauge is on the extreme right of the table on the right. The d.c. microammeter is in the center of this table. Behind the microammeter is the large metal box housing the ultraviolet lamp. The galvanometer lamp and ground glass scale are on the left front corner of this table. The galvanometer is over two meters to the right of the scale and is outside of the picture.

PROCEDURE

As soon as the glass joint had cooled down after the experimental tube had been sealed onto the vacuum system, the mechanical fore pump was turned on. This kept the pressure inside the tube and vacuum system at a pressure of about 15 microns of mercury for several days while the large oven and other apparatus were assembled. The system was examined with a freon leak detector and no leaks were found.

When the apparatus was assembled, the oil diffusion pump heater was turned on and the pressure was reduced to about 1×10^{-5} millimeters of mercury. When the pump was first turned on, the fore pressure rose to about 80 microns of mercury and then slowly dropped back down to about 15 microns. Then a trial bakeout run was made for about seven hours. Most of this time was spent in adjusting the voltages to the different oven heating elements to find the best arrangement to get a temperature of 400°C. The ovens were at a temperature of 400°C for about an hour and a half before they were turned off. The fore pressure rose to about 20 microns of mercury during the bakeout, indicating that gas was released.

When the ovens had cooled to room temperature, the pressure was found to have increased to 3.5×10^{-5} millimeters of mercury instead of decreasing. The aluminum evaporators were outgassed by heating the coils around the aluminum until the aluminum started to melt. One of the three coils burned out when too much voltage was applied accidentally.

At first it was thought that the pressure increase was due to too much gas adsorbed on the copper foil in the cold trap, so it was baked at 400°C for another three hours. Then when it had cooled to room temperature, a mixture of dry ice and acetone in a Dewar flask was brought up around it. The VG-2 ionization gauge showed that the pressure on the diffusion pump side of the cold trap had dropped to 2.125×10^{-6} millimeters of mercury, but the VG-1A showed the pressure in the experimental tube was 3.9×10^{-5} millimeters of mercury. Then the dry ice and acetone mixture was removed and the pressure stayed about the same. This showed that the copper foil in the cold trap was just as effective whether or not it was refrigerated.

Since the pressure in the tube was more than ten times greater than the pressure near the diffusion pump, it appeared that perhaps the copper was blocking or greatly slowing the flow of the air out of the tube and toward the diffusion pump. Therefore another attempt was made to drive it through. The tube was baked at 400°C for 12 hours and then the oven on the trap was turned on too. Both ovens were then kept at about 400°C for another 17 hours.

When the ovens had cooled to room temperature, it was found that the pressure near the diffusion pump was 2.4×10^{-6} millimeters of mercury, about the same as before the long bakeout, while the pressure in the tube had risen to about 7.6×10^{-5} millimeters of mercury. The pressure in the tube was therefore about 13 times the pressure at the diffusion pump. This indicated that only a very small leak

in the tube or ionization gauge could account for this pressure difference since these bakeouts should decrease the pressure. The suspected location for the leak was along the metal to glass seals around the leads into the tube. These were tested by rubbing a little castor oil around each of the leads. When the castor oil was rubbed onto one of the button seals, the pressure suddenly dropped. The castor oil had plugged the leak. This particular button seal had been struck accidentally when the oven was being built around the tube. The leak was permanently plugged by painting a little glyptal over it.

Soon after the leak was stopped, the pressure dropped to about 1×10^{-6} millimeters of mercury in the tube and about 6×10^{-7} millimeters of mercury at the diffusion pump.

It was assumed that the copper in the trap had adsorbed much of the air coming through the leak, so it was baked at 400°C for about three hours. During the bakeout the pressure in the tube rose to about 2×10^{-5} millimeters of mercury and the pressure at the diffusion pump rose accordingly. This indicated that an appreciable amount of gas was being removed from the copper. After the bakeout the pressure slowly dropped to about 4.1×10^{-7} millimeters of mercury at both gauges.

At this point the aluminum from one of the evaporators was evaporated to form the collecting electrode. At the same time some of the aluminum was deposited on the emitting electrode. The pressure slowly dropped to about 2.3×10^{-7} millimeters of mercury at the tube

and 3×10^{-7} millimeters of mercury at the diffusion pump. This pressure difference indicated that the aluminum surface in the tube was acting as a getter or the copper foil in the trap was behaving either as an obstruction to gas flowing back from the diffusion pump to the tube or as an additional pump. The fore pressure varied from about 17 microns down to 10 microns during the last bakeout and after.

In the meantime an attempt was made to balance the amplifier circuit under operating conditions, i.e., with the light source, potentiometer circuit, and galvanometer in operation. It was quite obvious that the grid of the amplifier tube was picking up electromagnetic waves from some source, since the galvanometer measuring the output of the amplifier would not settle down to a steady reading. As soon as the ultraviolet light source was turned off, the galvanometer settled down and the amplifier was balanced.

In order to stop the electromagnetic waves, the light source was put into a grounded metal box with a couple of small holes for the light to come through. This did not completely stop the interference, since some of it was apparently fed back into the 60 cycle, 110 volt power line and therefore it was fed to all of the other equipment operating on this power supply. Fortunately, the light source could be operated on direct current at 110 volts as well as on alternating current. It was connected to a direct current generator through shielded leads and the other equipment was left

on alternating current. This solved the problem and the amplifier was balanced with the light source on.

Shortly after the aluminum was evaporated, run 1 was taken and following at intervals of four and six hours were runs 2 and 3. The data taken included a record of the light intensity, the setting of the Ayrton shunt, galvanometer zero, galvanometer reading, and the applied retarding potential.

Runs 4 and 5 followed at intervals of about 12 hours each. After run 5 was taken, the filament of one of the evaporators was heated until the pressure rose to 1×10^{-6} millimeters of mercury and then cooled down. The pressure soon returned to its original value and then run 6 was taken. Runs 7, 8, and 9 followed at 24 hour intervals. Before run 7 was started, the position of the ultraviolet light source was adjusted since it apparently had gotten slightly out of line.

The air remaining in the tube was contaminating the emitter, but the process was rather slow. Therefore, immediately after run 9, the oven on the trap was warmed until the pressure reached about 1.2×10^{-5} millimeters of mercury and was held there for five minutes. This was done to speed up the contaminating rate. In about an hour and a half the pressure returned almost to its former value and then run 10 was taken.

Eight days later, the pressure was found to be about the same as before. Then more aluminum was evaporated from a second evaporator, and run 11 was taken on this new surface. Just before

run 11 was started, the position of the ultraviolet light source was adjusted again to get it back in line. Immediately after this run, the trap was heated until the pressure reached 1.3×10^{-5} millimeters of mercury and was held there for one minute. In about an hour and a half the pressure returned almost to its former value and run 12 was taken.

Five days later, run 13 was taken. Immediately after the run, the pressure was checked and found to be almost the same as before the runs were started. The VG-1A ionization gauge recorded about 3.5×10^{-7} millimeters of mercury. The VG-2 ionization gauge recorded about 5.0×10^{-7} millimeters of mercury, and the thermocouple gauge recorded about 12 microns of mercury.

RESULTS

The experimental curves were obtained by plotting $\log_{10}(I/x)$ against -x. Since the temperature was constant, the T^2 term was included in the constant $B_1 = \log_{10} \alpha A T^2$ in the equation

$$\log_{10}(I/x) = B_1 + \chi(x-x_o)$$

where $\chi(x-x_o)$ is the same as in the Introduction.

Figure 15 shows the method used in analyzing the data. The experimental curve was shifted until the best possible fit (by eye) to the theoretical curve was obtained. The horizontal shift is equal to x_o and the vertical shift equals B_1.

Figure 16 shows how well the data for a freshly evaporated surface fits the theoretical curve. At about $(x_o-x) \geqq 8$, the experimental points rise above the theoretical curve. This happens to be the region at which the emitted electrons due to the 2654 Angstrom line begin to reach the collecting electrode, so there is more current being collected.

Figure 17 shows how the data for a contaminated surface fits the theoretical curve. Again, the 2654 Angstrom line becomes effective in the region of $(x_o-x) \geqq 8$. Also, the data does not fit the theoretical curve in the vicinity of the maximum retarding potential, but drops below it. Thein (9, pp. 290-291) and Roehr (7, pp. 866-871) mention this effect for both high temperature and contamination.

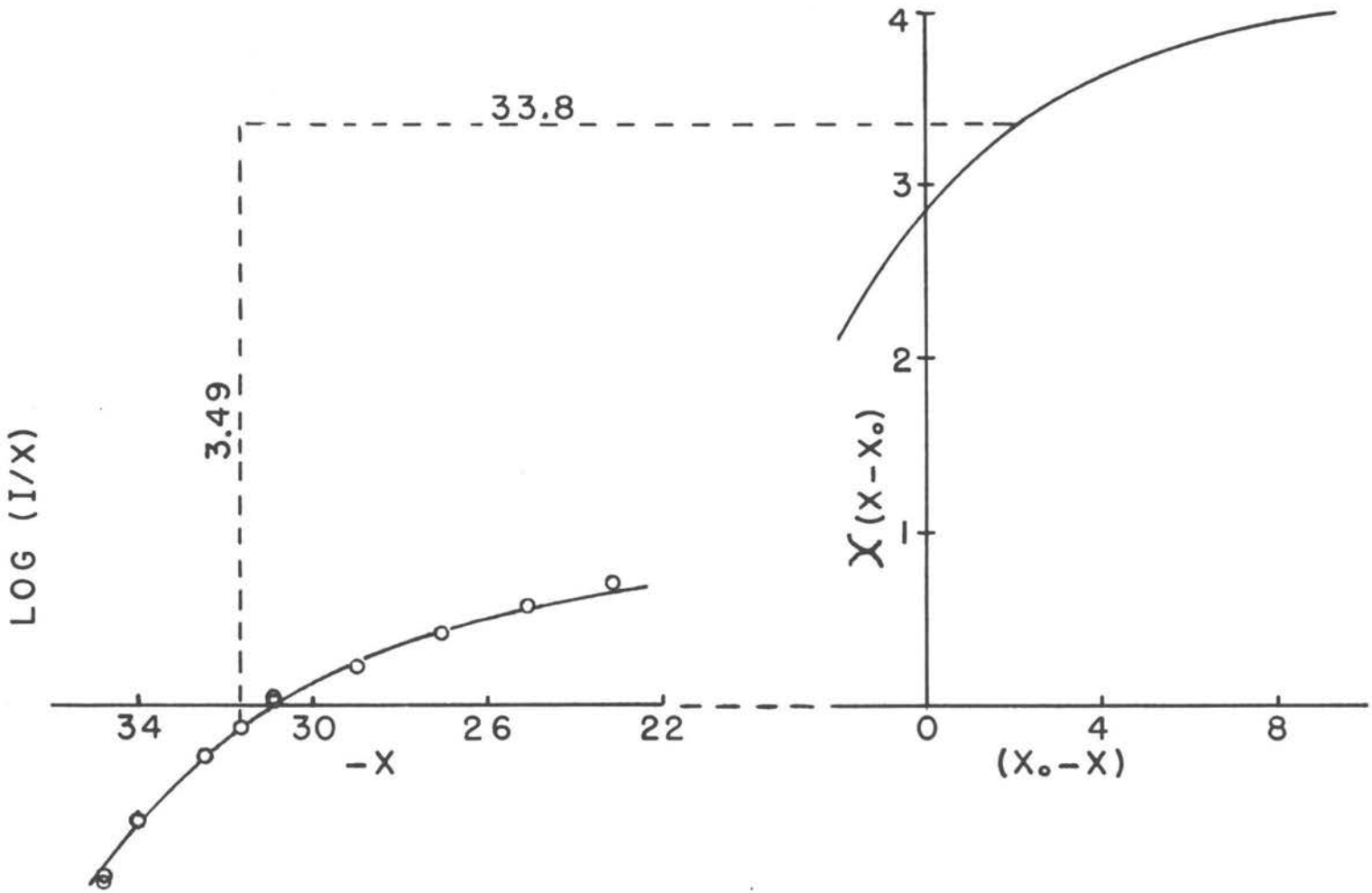

FIGURE 15. GRAPH OF RUN II SHOWING METHOD OF SUPERPOSITION.

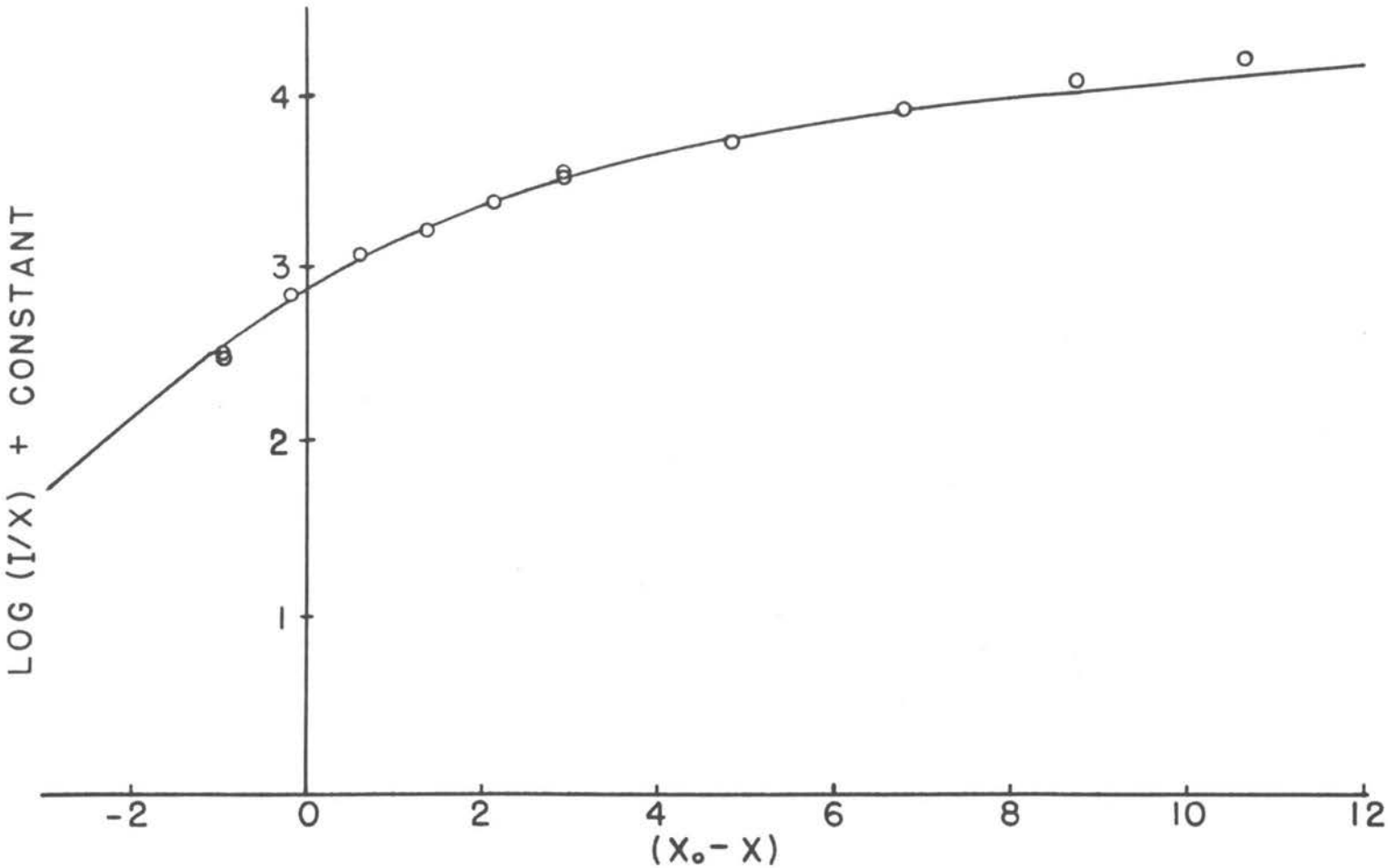

FIGURE 16. GRAPH OF RUN II SUPERPOSED ON THE THEORETICAL CURVE.

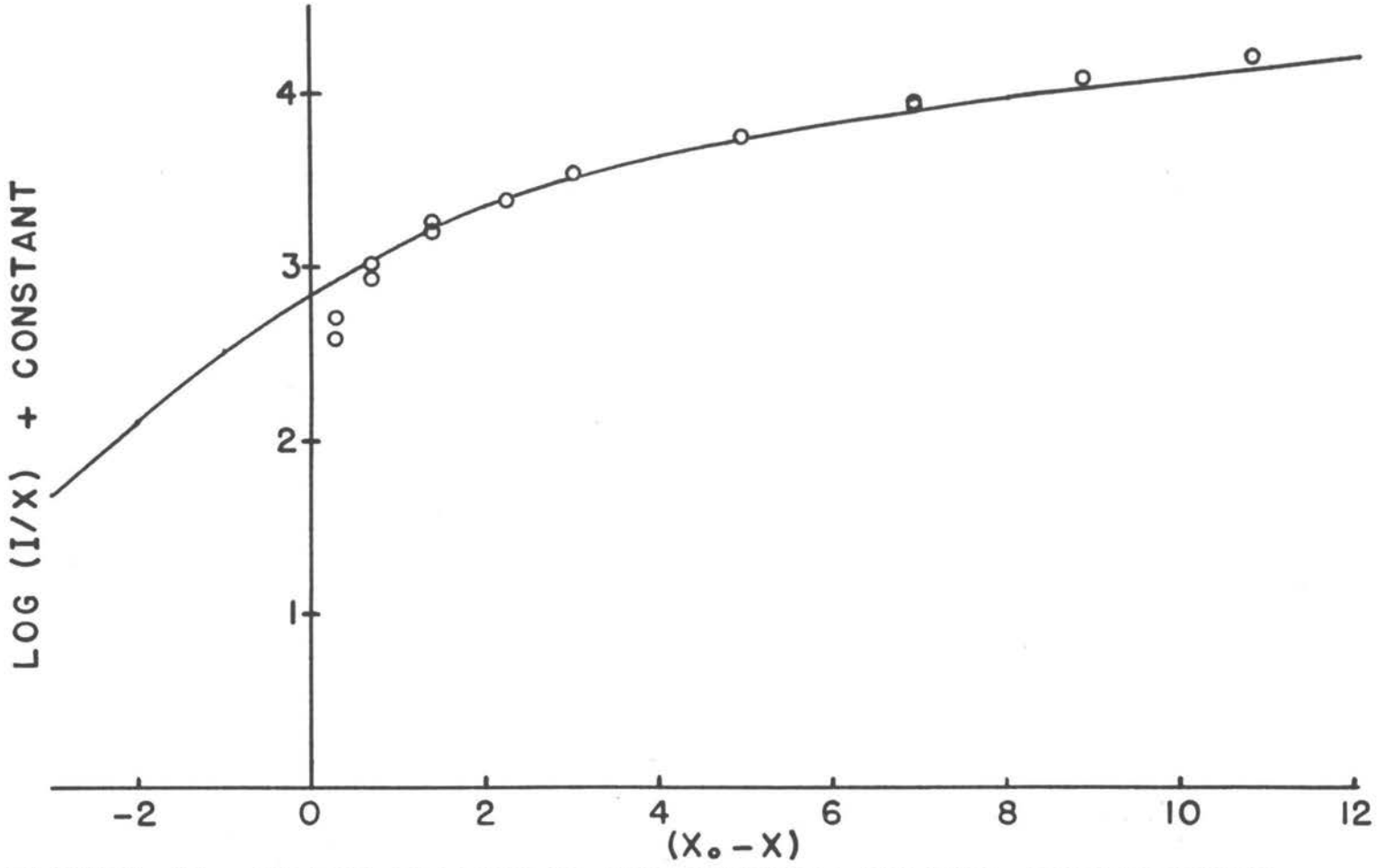

FIGURE 17. GRAPH OF RUN 12 SUPERPOSED ON THE THEORETICAL CURVE.

The runs are summarized in Table 1. The column headed Treatment indicates the length of time between runs and any changes introduced into the system. It was assumed that the increase in contamination is proportional to the length of time between runs. Also, any increase in the air pressure in the tube would increase the rate of contamination.

The column headed x_o gives the horizontal shift necessary to superpose the data on the theoretical curve. The next column gives the values of $V_m = x_o \frac{kT}{e}$. From this is found the work function $\phi = \frac{h\nu}{e} - V_m$. The last column gives the vertical shift necessary to superpose the data on the theoretical curve.

There was a general decrease in the work function from run 1 to run 10, which indicates that the surface was being contaminated. There was no valid data for run 3 because the batteries for the amplifier tube ran down and reduced considerably the sensitivity of the amplifier circuit. Fresh batteries were put into the circuit and run 4 was taken. Apparently the amplifier circuit was not yet properly adjusted to the fresh batteries, since the work function appears to have increased instead of decreasing. It was properly balanced when run 5 was taken.

When the surface was freshly evaporated, the work function increased and as the surface was contaminated it decreased again.

There was an over-all increase in the vertical shift B_1 from run 1 to run 10 and again from run 11 to run 13. The sudden decrease

Run	Treatment	x_o	V_m(volts)	∅(volts)	B_1
1	freshly evaporated surface	30.0	.776	4.114	3.60
2	4 hour interval	30.2	.782	4.108	3.60
3	6 hour interval				
4	12 hour interval	28.8	.745	4.145	3.50
5	12 hour interval	30.6	.792	4.098	3.60
6	pressure increased to 1×10^{-6} mm Hg and reduced to former value	30.8	.797	4.093	3.50
7	24 hour interval; position of light source adjusted	32.8	.849	4.041	3.65
8	24 hour interval	34.4	.890	4.000	3.66
9	24 hour interval	34.2	.885	4.005	3.66
10	pressure increased to 1.2×10^{-5} mm Hg and reduced to former value	43.5	1.126	3.764	3.80
11	8 days later; freshly evaporated surface; position of light source adjusted	33.8	.875	4.015	3.49
12	pressure increased to 1.3×10^{-5} and reduced again to former value	45.5	1.177	3.713	3.59
13	5 days later	49.0	1.268	3.622	3.60

Table 1. Summary of Runs

in the vertical shift for run 6 may be due to the possibility that the light source was slightly out of line. It was necessary to adjust the position of the light source before run 7 was taken. There may also have been some small fluctuations in the sensitivity of the amplifier.

The important result to be noted is that there is an over-all increase in the vertical shift when the work function decreases. Since A and T^2 are constants, the change in B_1 must be due to a change in α. Therefore, as the contamination increases through the small range considered here, the probability of emission also increases, but only by a relatively small amount as compared to the decrease in work function.

BIBLIOGRAPHY

1. Alpert, Daniel. Copper isolation trap for vacuum systems. The review of scientific instruments 24:1004-1005. 1953.

2. DuBridge, Lee Alvin and Hart Brown. An improved d.c. amplifying circuit. The review of scientific instruments 4:532-536. 1936.

3. DuBridge, Lee Alvin. New theories of the photoelectric effect. Paris, Hermann and Cie, Éditeurs, 1935. 56 p. (Actualités scientifiques et industrielles. No. 268).

4. DuBridge, Lee Alvin. Theory of the energy distribution of photoelectrons. The physical review 43:727-741. 1933.

5. Fowler, R. H. The analysis of photoelectric sensitivity curves for clean metals at various temperatures. The physical review 38:45-56. 1931.

6. Mann, Marvin Mellard, Jr. and Lee Alvin DuBridge. The absolute photoelectric yields of Mg, Be and Na. The physical review 51:120-124. 1937.

7. Roehr, Walter W. The effect of temperature on the energy distribution of photoelectrons. II Total energies. The physical review 44:866-871. 1933.

8. Strong, John Donovan. Procedures in experimental physics. New York, Prentice Hall, 1938. 642 p.

9. Thein, Louis Peter. The photoelectric sensitization of aluminum. The physical review 53:287-292. 1938.